A new study of the polarized parton densities in the nucleon

Elliot Leader

Birkbeck College, University of London

Malet Street, London WC1E 7HX, England

E-mail: e.leader@physics.bbk.ac.uk

Aleksander V. Sidorov

Bogoliubov Theoretical Laboratory

Joint Institute for Nuclear Research

41980 Dubna, Russia

E-mail: sidorov@thsun1.jinr.ru

Dimiter B. Stamenov

Institute for Nuclear Research and Nuclear Energy

Bulgarian Academy of Sciences

blvd. Tsarigradsko Chaussee 72, Sofia 1784, Bulgaria

E-mail:stamenov@inrne.bas.bg

Abstract

We present a new next-to-leading order QCD analysis of the world data on inclusive polarized deep inelastic lepton-nucleon scattering adding to the old set of data the final SMC results, the HERMES proton and very recent SLAC/E155 deuteron data. We find an excellent fit to the data and present results for the polarized parton densities in different factorization schemes. These results are in a good agreement with what follows from the theory. We have also found that the main effect of the newly incorporated data is a better determination of the polarized gluon density.

Recently [1, 2] we carried out a next-to-leading order (NLO) QCD analysis of the world data on polarized inclusive deep inelastic scattering (DIS). Since then the SMC group at CERN have re-analyzed their small-x data, using a totally new method of analysis, and published the final results of their experiment [3]. At the same time new data have emerged from the HERMES Collaboration at DESY [4] and very recently from the E155 experiment at SLAC [5].

The SMC group have themselves carried out an NLO QCD analysis [6] based on their final results and most of the world data available at that time (with the exception of the final results from the SLAC/E143 experiment [7]). Given that there are significant changes in the SMC data, and the high precision of the new HERMES and SLAC/E155 data, we felt it necessary to redo our analysis.

We have found that the newly incorporated data improve the determination of the polarized parton densities, in particular, of the poorly known gluon density. In this letter we present a brief summary of the general trends in our new results as well as a concise description of our present knowledge of the polarized parton densities.

All details of our approach are given in [1, 2]. Here we simply recall that we carry out our analysis in three different factorization schemes: $\overline{\mathrm{MS}}$, AB (Adler-Bardeen) [8] and JET [9]. We then test the stability of our analysis by comparing densities in one scheme, as determined from the fit to the data, with these same densities evaluated using the transformation rules connecting densities in different schemes.

We prefer to work with separate valence and sea parton densities and we check the stability of our results when we vary the parameter λ corresponding to different flavour decompositions of the sea

$$\Delta\bar{u} = \Delta\bar{d} = \lambda\Delta\bar{s} \ , \tag{1}$$

i.e., we confirm that the non-singlets $\Delta q_3, \ \Delta q_8,$ the singlet $\Delta\Sigma$ and the gluon density ΔG are invariant. Note that this implies that the strange quark density

$$\Delta\bar{s} = \frac{1}{6}(\Delta\Sigma - \Delta q_8) \ , \tag{2}$$

is also invariant (does *not* change as λ is varied) and it can be extracted from the data as well as $\Delta\Sigma$. Of course, the valence quark densities Δu_v and Δd_v are sensitive to the different assumptions about the sea. Nonetheless they are of interest for predicting the behaviour of other processes, e.g., polarized semi-inclusive DIS, polarized Drell-Yan reactions, etc.

For the input polarized parton densities at $Q_0^2 = 1\ GeV^2$ we have adopted a very simple parametrization

$$\begin{aligned}
\Delta u_v(x, Q_0^2) &= \eta_u A_u x^{a_u} x u_v(x, Q_0^2) \ , \\
\Delta d_v(x, Q_0^2) &= \eta_d A_d x^{a_d} x d_v(x, Q_0^2) \ , \\
\Delta Sea(x, Q_0^2) &= \eta_S A_S x^{a_S} x Sea(x, Q_0^2) \ , \\
\Delta G(x, Q_0^2) &= \eta_g A_g x^{a_g} x G(x, Q_0^2) \ ,
\end{aligned} \tag{3}$$

where on RHS of (3) we have used the MRST unpolarized densities [10]. The normalization factors A_f in (3) are fixed such that η_f are the first moments of the polarized densities.

The first moments of the valence quark densities η_u and η_d are fixed by the octet nucleon and hyperon β decay constants [11]

$$g_A = F + D = 1.2573\ \pm\ 0.0028, \quad a_8 = 3F - D = 0.579\ \pm\ 0.025\ , \tag{4}$$

and in the case of SU(3) flavour symmetry of the sea ($\Delta\bar{u} = \Delta\bar{d} = \Delta\bar{s}$ at Q_0^2)

$$\eta_u = 0.918\ , \qquad \eta_d = -0.339\ . \tag{5}$$

The rest of the parameters in (3),

$$\{a_u,\ a_d,\ \eta_S,\ a_S\ ,\ \eta_g\ , a_g\}\ , \tag{6}$$

have been determined from the best fit to the $A_1^N(x, Q^2)$ data.

The numerical results of our fits to the world data on $A_1^N(x, Q^2)$ [3-5, 7, 12-15] are summarized in Table 1. The data used (161 experimental points) cover the following kinematic region:

$$0.004 < x < 0.75, \qquad 1 < Q^2 < 72\ GeV^2\ . \tag{7}$$

As in our previous analyses [1, 2] the total (statistical and systematic) errors are taken into account. The results presented in Table 1 correspond to an SU(3) symmetric sea. Note that in this case $a_{\bar{s}} = a_S$ and the first moment of the strange sea quarks, $\eta_{\bar{s}} \equiv \Delta\bar{s}(1, Q_0^2) = \eta_S/6$.

It is seen from the Table 1 that the values of χ^2/DOF coincide almost exactly in the different factorization schemes, which is a good indication of the stability of the analysis. The NLO QCD predictions are in a very good agreement with the presently available data on A_1^N and g_1^N, as is illustrated in the JET scheme fit in Figs. 1a-c.

Table 1. Results of the NLO QCD fits in the JET, AB and $\overline{\rm MS}$ schemes to the world A_1^N data ($Q_0^2 = 1\ GeV^2$). The errors shown are total (statistical and systematic).

Scheme	JET	AB	$\overline{MS}$
DOF	161 - 6	161 - 6	161 - 6
χ^2	128.3	128.4	129.4
χ^2/DOF	0.828	0.828	0.835
a_u	0.276 $\pm$ 0.030	0.278 $\pm$ 0.031	0.257 $\pm$ 0.024
a_d	0.077 $\pm$ 0.135	0.065 $\pm$ 0.136	0.179 $\pm$ 0.107
$a_{\bar{s}}$	1.524 $\pm$ 0.391	1.668 $\pm$ 0.403	0.761 $\pm$ 0.188
$\eta_{\bar{s}}$	- 0.032 $\pm$ 0.005	- 0.029 $\pm$ 0.006	- 0.051 $\pm$ 0.006
a_g	0.175 $\pm$ 0.452	0.144 $\pm$ 0.417	3.6 $\pm$ 3.8
η_g	0.57 $\pm$ 0.14	0.58 $\pm$ 0.12	0.07 $\pm$ 0.10
$\Delta\Sigma(1)$	0.389 $\pm$ 0.037	0.407 $\pm$ 0.044	0.275 $\pm$ 0.044
$a_0(1\ GeV^2)$	0.26 $\pm$ 0.05	0.27 $\pm$ 0.05	0.28 $\pm$ 0.04

Let us now comment briefly upon the state of our knowledge about the individual polarized parton densities. The extracted quark (valence and sea) and gluon densities at $Q_0^2 = 1\ GeV^2$ are shown in Fig. 2 and Fig. 3, respectively.

$\mathbf{\Delta u_v(x, Q^2)}$ and $\mathbf{\Delta d_v(x, Q^2)}$

i) The valence quark densities are practically unchanged if the new (final SMC, HERMES proton and SLAC/E155 deuteron) data are incorporated in the analysis. (Note that Δu_v is very well determined once an assumption about the flavour decomposition of the sea is made.)

ii) Δu_v and Δd_v in the JET, AB and $\overline{\rm MS}$ schemes coincide within the errors, in excellent agreement with what follows from the theory (they should be the same in the factorization schemes under consideration).

iii) Although the first moment of $\Delta d_v(x, Q_0^2)$, η_d, has been kept fixed in the analysis (see Eq. (5)), the parameter a_d, and therefore Δd_v is not well determined from the present data (see Fig. 2).

$\mathbf{\Delta\bar{s}(x, Q^2)}$ and $\mathbf{\Delta\Sigma(x, Q^2)}$

Note that these quantities are scheme dependent.

i) $\Delta\bar{s}$ and $\Delta\Sigma$ are well determined from the data now (see Fig. 2).

ii) The first moments $\eta_{\bar{s}}$ in the JET and AB schemes are in a very good agreement. The same is valid for the first moments $\Delta\Sigma(1)$ (see Table 1). (We recall that according to the definition of the JET and AB schemes $\Delta\Sigma(1)$ as well as $\eta_{\bar{s}}$ should be the same in both schemes.) The corresponding densities $\Delta\bar{s}(x,Q^2)$ and $\Delta\Sigma(x,Q^2)$ in both schemes are slightly different because their higher moments are not equal.

iii) The first moment of $\Delta\bar{s}$ in the $\overline{\mathrm{MS}}$ scheme, $(\eta_{\bar{s}})_{\overline{\mathrm{MS}}}$, is almost twice as big as it is in the JET(AB) schemes, $(\eta_{\bar{s}})_{\mathrm{JET(AB)}}$:

$$(\eta_{\bar{s}})_{\overline{\mathrm{MS}}} = -0.051 \pm 0.006, \qquad (\eta_{\bar{s}})_{JET} = -0.032 \pm 0.005. \tag{8}$$

The polarized strange quark density is significantly different from zero independently of the factorization schemes used in the analysis. The result (8) demonstrates the extent to which the strange quark densities in different schemes can differ in the polarized case.

Gluons $\mathbf{\Delta G(x, Q^2)}$

i) The new set of data allows a better determination of the polarized gluon density in the JET and AB schemes.

In previous studies χ^2 was quite insensitive to the value of a_g in all factorization schemes under consideration, and the results of the fits corresponding to fixing $a_g = 0.6$ were presented in [1, 2]. The results when a_g is a free parameter are summarized in Table 2.

Table 2. The values of the parameters associated with the input polarized gluon density in the JET, AB and $\overline{\mathrm{MS}}$ schemes for the new and old sets of data.

Param.	Data set	JET	AB	$\overline{\mathrm{MS}}$
a_g	old	1.8 ± 2.1	1.7 ± 1.8	1.6 ± 1.9
η_g	old	0.24 ± 0.35	0.28 ± 0.40	0.30 ± 0.50
a_g	new	0.18 ± 0.45	0.14 ± 0.42	3.6 ± 3.8
η_g	new	0.57 ± 0.14	0.58 ± 0.12	0.07 ± 0.10

It is clear from the Table 2 that now both the value of a_g and η_g, i.e., the shape and the normalization of the gluon density are much better constrained in the JET and AB schemes. The progress in extracting the polarized gluon density from the new data set is illustrated in Fig. 3 (JET scheme).

ii) In the $\overline{\mathrm{MS}}$ scheme the gluons are still poorly constrained. χ^2 continues to be insensitive to a large range of possible values for a_g (see Table 2). The obtained value of η_g in this case is consistent with zero. However, if we fit the data with a fixed value of $a_g = 0.2$ (in accord with the values obtained in the JET, AB schemes), we find $\eta_g = 0.62 +/- 0.42$, in agreement with the values of this quantity in the JET and AB schemes, as expected theoretically.

Axial charge $\mathbf{a_0(Q^2)}$

i) The good agreement between the values of $a_0(Q^2)$ determined in the different schemes is demonstrated in Table 1, which illustrates how our analysis respects the scheme-independence of physical quantities.

ii)The central values of a_0 at $Q^2 = 1\ GeV^2$ are slightly smaller than the corresponding values obtained from our previous analysis.

We have also investigated the sensitivity of χ^2 to the alternative possibilities of explanation of the spin of the nucleon via the spins of its constituents, namely:

i) $\eta_{\bar{s}} \neq 0,\ \eta_g = 0$, so that $a_0 \approx \Delta\Sigma\ <<\ a_8 = 0.58$

ii) $\eta_{\bar{s}} = 0,\ \eta_g \neq 0$, so that $a_0\ <<\ \Delta\Sigma \approx a_8 = 0.58$

iii) $\eta_{\bar{s}} \neq 0,\ \eta_g \neq 0$

The numerical results (JET scheme) are given in Table 3.

Table 3. Sensitivity of χ^2 to the absence of polarized strange quarks $\Delta\bar{s}$ or gluons ΔG at $Q^2 = 1\ GeV^2$.

Assumption	χ^2	$-\ \eta_{\bar{s}}$	η_g	a_0
$\eta_{\bar{s}} \neq 0,\ \eta_g = 0$	133.1	0.065 ± 0.014	0	0.19 ± 0.09
$\eta_{\bar{s}} = 0,\ \eta_g \neq 0$	134.7	0	1.33 ± 0.11	0.27 ± 0.04
$\eta_{\bar{s}} \neq 0,\ \eta_g \neq 0$	128.3	0.032 ± 0.005	0.57 ± 0.14	0.26 ± 0.05

It is seen from the Table that the present inclusive DIS data prefer small strange quark and small gluon polarized densities at $Q^2 = 1\ GeV^2$:

$$\eta_{\bar{s}} = -0.032 \pm 0.005, \quad \eta_g = 0.57 \pm 0.14. \tag{9}$$

First moments of the spin structure functions

Finally, we present our results for the first moments of the nucleon spin structure functions g_1^N at $Q^2 = 5\ GeV^2$ in the measured x range from 0.003 to 0.8 (AB scheme):

$$\int_{0.003}^{0.8} dx g_1^N(x, Q^2 = 5\ GeV^2)_{fit} \quad = \quad \begin{array}{rl} 0.133 & \text{for Proton} \\ 0.039 & \text{for Deuteron} \\ -0.048 & \text{for Neutron} \end{array} \tag{10}$$

which are in excellent agreement with their experimental values [6] obtained from the world set of data (HERMES proton and E155 deuteron data not included):

$$\begin{array}{rlllll} 0.130 & \pm\ 0.003(stat) & \pm\ 0.005(syst) & \pm\ 0.004(evol) & \text{for Proton} \\ 0.036 & \pm\ 0.004(stat) & \pm\ 0.003(syst) & \pm\ 0.002(evol) & \text{for Deuteron} \\ -0.054 & \pm\ 0.007(stat) & \pm\ 0.005(syst) & \pm\ 0.004(evol) & \text{for Neutron} \end{array} \tag{11}$$

The nucleon spin

In the JET and AB schemes it is meaningful to interpret $\Delta\Sigma(1)$, the first moment of the singlet density $\Delta\Sigma(x, Q^2)$, as the contribution of the quark spins to the nucleon's spin. Our value of $\Delta\Sigma = 0.40 \pm 0.04$ is not far from the value 0.6 expected in certain quark models [16]. For the spin contribution from both quarks and gluons we have (JET scheme):

$$\frac{1}{2}\Delta\Sigma(1) + \eta_g = 0.76 \pm 0.14 \tag{12}$$

This value is consistent with 1/2 in two standard deviations. The more accurate determination of $\Delta\Sigma$ and η_g will answer the basic question how the spin of nucleon is divided up among the spin of quarks and gluons and their orbital angular momenta.

In conclusion, we have re-analyzed the world data on inclusive polarized deep inelastic lepton-nucleon scattering in NLO QCD adding to the old set of data the final SMC results, the new HERMES proton and SLAC/E155 deuteron data. As in the previous analysis it was demonstrated that the polarized DIS data are in an excellent agreement with the pQCD predictions for $A_1^N(x, Q^2)$ and $g_1^N(x, Q^2)$ in all the factorization schemes considered. The polarized parton densities have been extracted from the data. We have found that the main effect of the newly incorporated data is a better determination of the polarized gluon density, but in comparison with the other densities the uncertainty is still large. It follows from our analysis that the present inclusive DIS data prefer small strange quark and small gluon polarized densities, but they are significantly different from zero.

To test more precisely the spin properties of QCD and to determine better the polarized densities, accurate data from both the inclusive (neutral and charged current) polarized DIS and the semi-inclusive processes in a larger kinematical region are needed. Finally, a direct measurement of the gluon polarization is necessary. We hope the COMPASS experiment at CERN, the future experiments at the hadron collider RHIC and the possibility of having a polarized proton beam at HERA will help to further a more profound study of the internal structure of the nucleon.

This research was partly supported by a UK Royal Society Collaborative Grant, by the Russian Foundation for Basic Research, Grant No 99-01-00091 and by the Bulgarian science Foundation under Contract Ph 510.

References

[1] E. Leader, A. V. Sidorov and D. B. Stamenov, Phys. Rev. D 58 (1998) 114028.

[2] E. Leader, A. V. Sidorov and D. B. Stamenov, Phys. Lett. B 445 (1998) 232.

[3] SMC, D. Adeva et al., Phys. Rev. D 58 (1998) 112001.

[4] HERMES Collaboration, A. Airapetian et al., Phys. Lett. B 442 (1998) 484.

[5] SLAC/E155 Collaboration, P. L. Anthony et al., SLAC-PUB-8401, March 1999, hep-ex/9904002.

[6] SMC, D. Adeva et al., Phys. Rev. D 58 (1998) 112002.

[7] SLAC E143 Collaboration, K. Abe et al., Phys. Rev. D 58 (1998) 112003.

[8] R. D. Ball, S. Forte and G. Ridolfi, Phys. Lett. B 378 (1996) 255.

[9] R. D. Carlitz, J. C. Collins and A.H. Mueller, Phys. Lett. B 214 (1988) 229;
M. Anselmino, A. V. Efremov and E. Leader, Phys. Rep. 261 (1995) 1;
D. Müller and O. V. Teryaev, Phys. Rev. D 56 (1997) 2607.

[10] A. D. Martin, R. G. Roberts, W. J. Stirling and R. S. Torn,
Eur. Phys. J. C 4 (1998) 463.

[11] Particle Data Group, L. Montanet et al., Phys. Rev. D 50 (1994) 1173;
F. E. Close and R. G. Roberts, Phys. Lett. B 313 (1993) 165.

[12] EMC, J. Ashman et al., Phys. Lett. B 206 (1988) 364;
Nucl. Phys. B 328 (1989) 1.

[13] SLAC E142 Collaboration, P. L. Anthony et al., Phys. Rev. D 54 (1996) 6620.

[14] SLAC/E154 Collaboration, K. Abe et al., Phys. Rev. Lett. 79 (1997) 26.

[15] HERMES Collaboration, K. Ackerstaff et al., Phys. Lett. B 404 (1997) 383.

[16] R. D. Jaffe and A. Manohar, Nucl. Phys. B 337 (1990) 509.

Figure Captions

Fig. 1. Comparison of our NLO results in the JET scheme for $A_1^N(x, Q^2)$ (a,b) and $xg_1^N(x, Q^2)$ (c) with the experimental data at the measured x and Q^2 values. Errors bars represent the total error.

Fig. 2. Next-to-leading order polarized valence, strange and singlet quark distributions at $Q^2 = 1\ GeV^2$ with their error bands (JET scheme). The systematic errors are added quadratically.

Fig. 3. Next-to-leading order polarized gluon density at $Q^2 = 1\ GeV^2$ determined from the old (a) and the new (b) world sets of data (JET scheme). The error bands account for the statistical and systematic uncertainties.

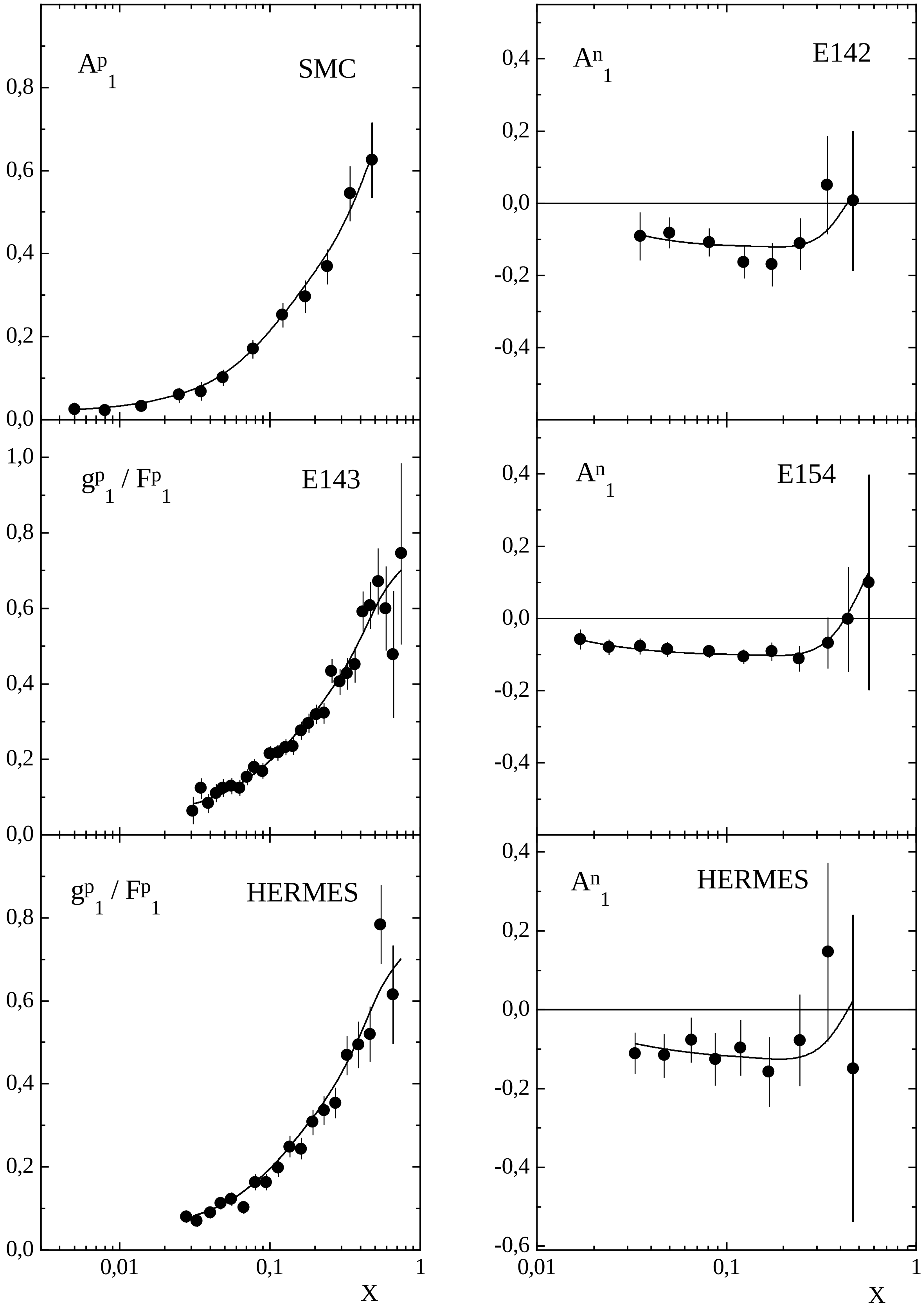

A^p_1
SMC
g^p_1 / F^p_1
E143
g^p_1 / F^p_1
HERMES
A^n_1
E142
A^n_1
E154
A^n_1
HERMES
0,0
0,2
0,4
0,6
0,8
1,0
-0,2
-0,4
-0,6
0,01
0,1
1
X

Fig. 1a

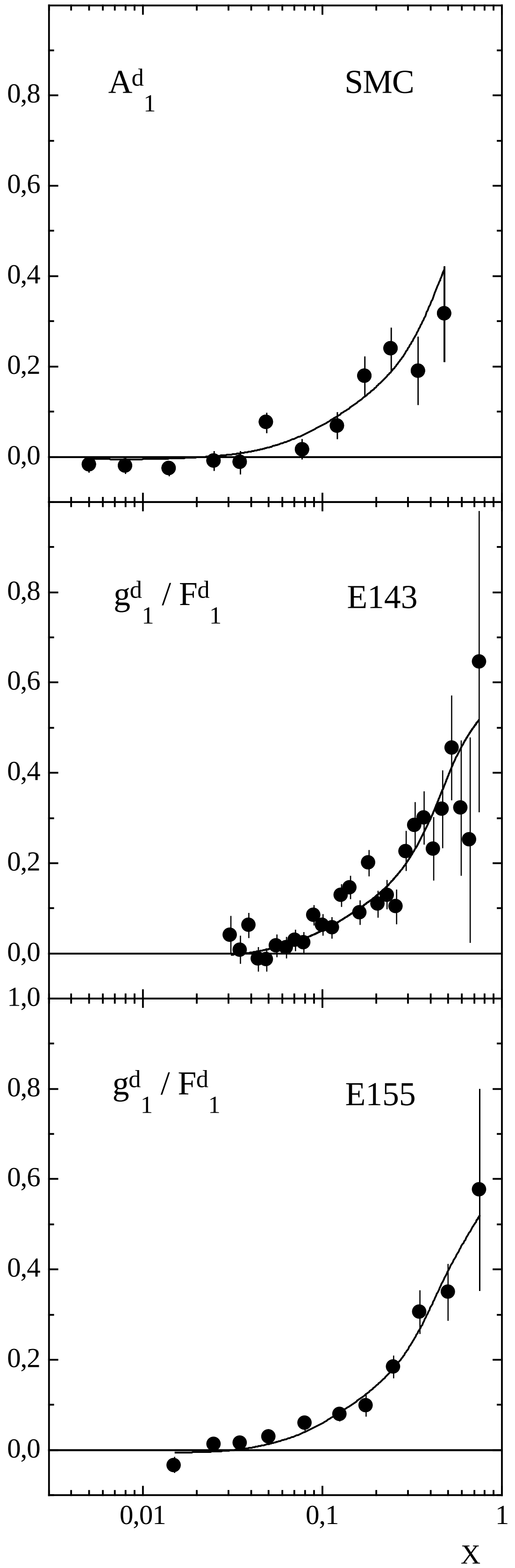

Fig. 1b

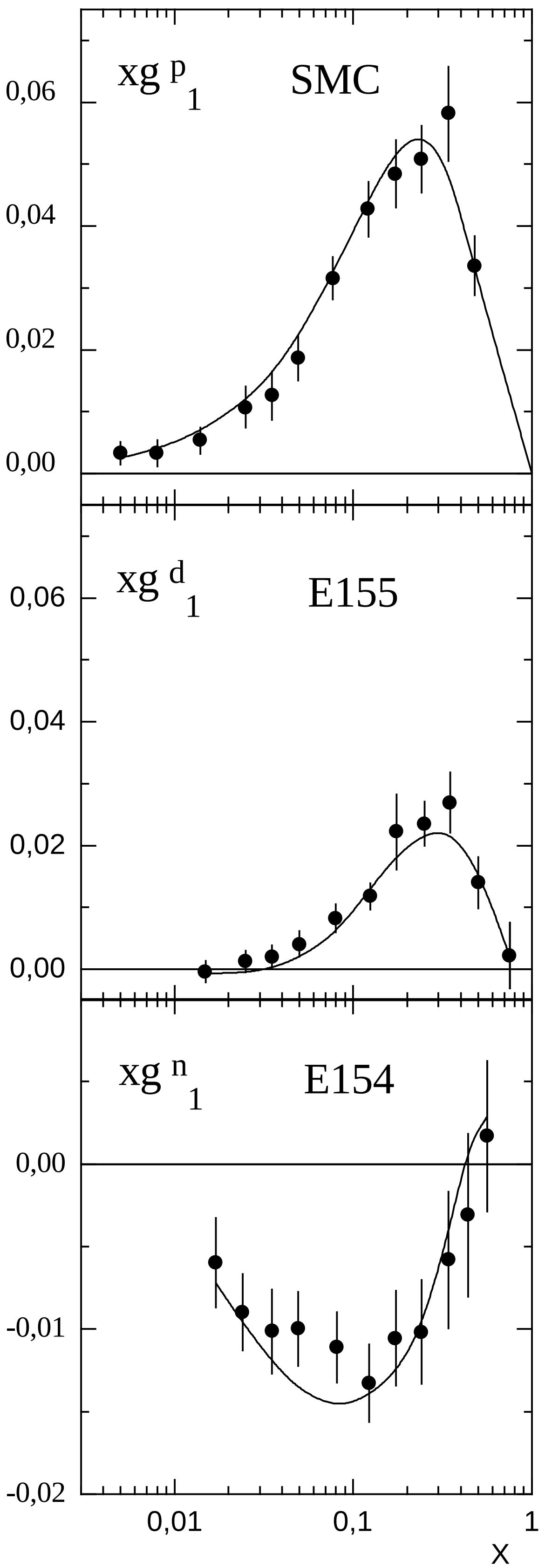

xg p 1
SMC
0,06
0,04
0,02
0,00
xg d 1
E155
0,06
0,04
0,02
0,00
xg n 1
E154
0,00
-0,01
-0,02
0,01
0,1
1
X

Fig. 1c

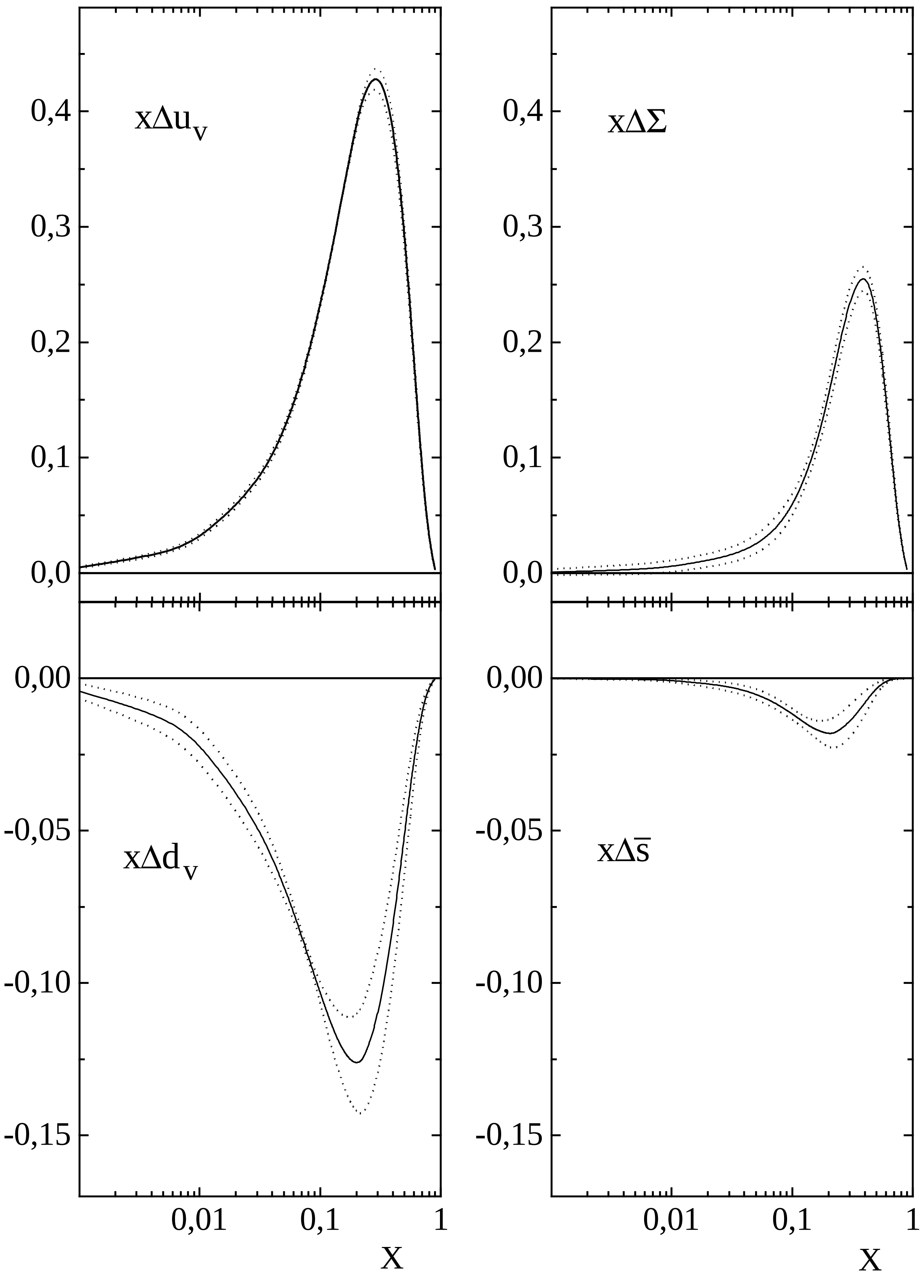
xΔu$_v$
x$\Delta\Sigma$
xΔd$_v$
x$\Delta\bar{s}$
0,4
0,3
0,2
0,1
0,0
0,00
-0,05
-0,10
-0,15
0,01
0,1
1
x

Fig. 2

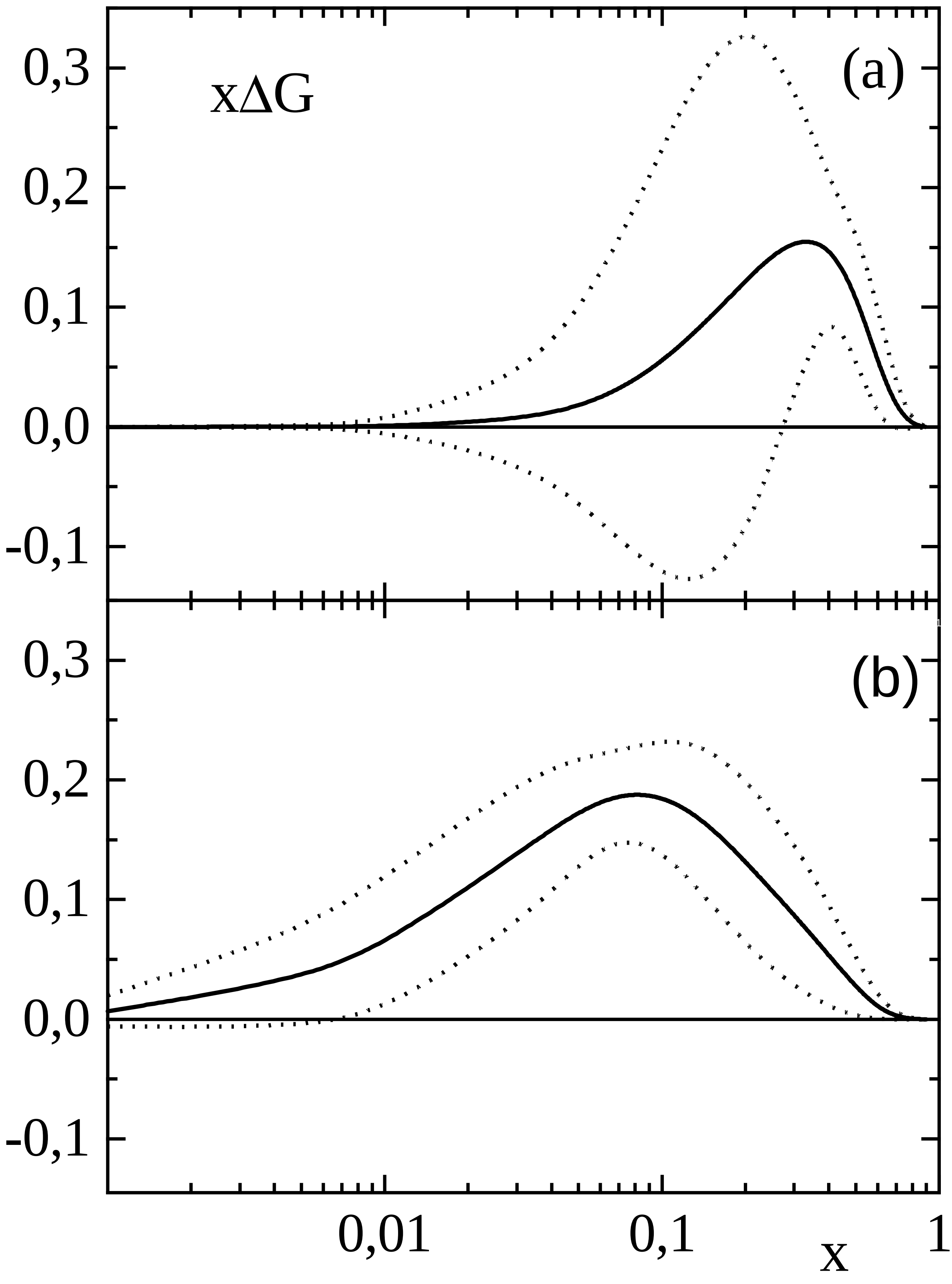

Fig. 3